Influence of droplets coverage on the electrochemical response of planar microelectrodes and potential solving strategies based on nesting concept

Yue Yu [1] , **Zhanming Li** Corresp. [2]

1 Department of Biosystems Engineering, Zhejiang University, Hangzhou, China

2 Department of Food Science, College of Life Science, China Jiliang University, Hangzhou, China

Corresponding Author: Zhanming Li
Email address: lizhanming@cjlu.edu.cn

Recently, biosensors have been widely used for the detection of bacteria, virus and other toxins. Electrodes, as commonly used transducers, are vital part of electrochemical biosensors. The coverage of the droplets can change significantly based on the hydrophobicity of the microelectrode surface materials. In the present research, screen-printed interdigitated microelectrodes (SPIMs), as one type of planar microelectrodes, were applied to investigate the influence of droplets coverage on electrochemical response. Furthermore, three dimensional (3D) printing technology was employed to print smart devices with different diameters based on nesting concept. Theoretical explanations were proposed to elucidate the influence of the droplets coverage on the electrochemical response. 3D-printed ring devices were used to incubate the SPIMs and the analytical performances of the SPIMs were tested. According to the results obtained, our device successfully improved the stability of the signal responses and eliminated irregular signal changes to a large extent. Our proposed method based on nesting concept provide a promising method for the fabrication of stable electrochemical biosensors . We also introduced two types of electrode bases to improve the signal stability.

1 **Influence of droplets coverage on the electrochemical response of planar microelectrodes**

2 **and potential solving strategies based on nesting concept**

3 Yue Yu[1], Zhanming Li[2*]

4 [1]Department of Biosystems Engineering, Zhejiang University, Hangzhou 310058, China.

5 [2]Department of Food Science, College of Life Science, China Jiliang University, Hangzhou
6 310012, China.

8 *Corresponding to: Dr. Zhanming Li, Phone: +86-571-86872488, Email:
9 lizhanming@cjlu.edu.cn
10   .

12   **Abstract**

13   Recently, biosensors have been widely used for the detection of bacteria, virus and other toxins.

14   Electrodes, as commonly used transducers, are vital part of electrochemical biosensors. The

15   coverage of the droplets can change significantly based on the hydrophobicity of the

16   microelectrode surface materials. In the present research, screen-printed interdigitated

17   microelectrodes (SPIMs), as one type of planar microelectrodes, were applied to investigate the

18   influence of droplets coverage on electrochemical response. Furthermore, three dimensional (3D)

19   printing technology was employed to print smart devices with different diameters based on

20   nesting concept. Theoretical explanations were proposed to elucidate the influence of the

21   droplets coverage on the electrochemical response. 3D-printed ring devices were used to

22   incubate the SPIMs and the analytical performances of the SPIMs were tested. According to the

23   results obtained, our device successfully improved the stability of the signal responses and

24   eliminated irregular signal changes to a large extent. Our proposed method based on nesting

25   concept provide a promising method for the fabrication of stable electrochemical biosensors. We

26   also introduced two types of electrode bases to improve the signal stability.

27   **1   Introduction**

28   Recently, biosensors have been widely used for the detection of bacteria, virus and other

29   toxins. Biosensors are analytical systems composed of a biological sensing element and a

30   physical transducer. The transducer is designed for the conversion of biological information into

31   a detectable signal, such as proton concentration, absorption or reflectance, light emission, mass

32   changes, and so on (Hunt and Armani, 2010; Lepinay et al., 2014; Olaru et al., 2014; Thévenot et

33 al., 2001; Van Dorst et al., 2010). Electrodes, as commonly used transducers, are vital part of

34 electrochemical biosensors. They are designed to transform the recognition of a biological

35 molecule into an easily quantifiable electrical signal (Gerard et al., 2002; Li et al., 2015b).

36 Electrodes with small dimensions, commonly referred to as microelectrodes, can maximize the

37 signal change, reduce the response time and work in a two-electrode system, thus benefiting the

38 fabrication and performance of electrochemical biosensors (Huey et al., 2012; Park and Beskok,

39 2008). Microelectrodes exhibit more accurate electrochemical response to low concentrations of

40 electro-active species in solution than large planar electrodes. Excellent flexibility and cycling

41 stability also promise potential applications in lab-on-a-chip systems (Ch et al., 2006; Huang et

42 al., 2009; Ueno et al., 2005).

43   Electrochemical biosensors based on planar microelectrodes have been described in many

44 literatures (Bernalte et al., 2011; Taleat et al., 2014; Valentini et al., 2014; Wang et al., 2012;

45 Zhu et al., 1998). The sensitivity and the signal-to-noise ratio of planar microelectrode can be

46 influenced by many factors, such as the diameter of the electrode, surface coverage, electrode

47 geometry and the electroactivity of analytes (Brett and Thiemann, 2002; Kostecki et al., 2000;

48 Liu et al., 2014; Xu et al., 2004; Zhu et al., 1998). The droplets exhibit different coverage on the

49 microelectrode surface, depending on the hydrophobicity of the microelectrode surface which

50 may trigger irregular signal change. The commonly-used incubation methods for planar

51 microelectrodes include dropping and immersing coatings. The influence of droplets coverage

52 which is important but less concerned, should be evaluated when dropping coating is used for

53   incubation. Screen-printed interdigitated microelectrodes (SPIMs), as one type of planar

54   microelectrodes, which may integrate the merits of screen printed microelectrodes and

55   interdigitated microelectrodes, have been used to develop sensitive, rapid-responding, cost-

56   effective biosensors (Li et al., 2015a). In this manuscript, we investigate the influence of droplets

57   coverage on the electrochemical response of SPIMs.

58   Three-dimensional (3D) printed devices have captured much attention in many fields,

59   including food safety and analysis (Sun et al., 2015; Wei et al., 2015; Xing et al., 2015). As we

60   know, many birds build nests to incubate their eggs and raise their young in a protective

61   environment (Vilé et al., 2015). In order to further analyze the influence of the droplets coverage

62   quantitatively, 3D printing technology was employed to print smart nest-like devices with

63   different diameters to keep the immobilization and detection within the devices based on nesting

64   concept. Both the theoretical analysis and our experimental results support our conclusion that

65   the droplets coverage has significant influence on the electrochemical response of biosensors.

66   Depending on the varying hydrophobic properties of the materials used to immobilize the

67   surface of the electrodes, the droplets can show gathering or dispersing properties (Costa et al.,

68   2015; Gryczan et al., 2015; Santoro et al., 2014). According to such principle, different materials

69   are developed to remodel the surface of the SPIMs to improve the stability of signal responses.

70   In the present research, ring devices around the detection area were designed to gather the

71   droplets. Silica gel was used as a mode sample to validate our methodology. 3D-printed ring

72   devices were used to incubate the SPIMs and the analytical performances of our device and

73   method were also evaluated. Software can also be used to handle the signal stability by electrode

74   base design.

2   Materials and methods

2.1   Reagents and apparatus

77   *E. coli* O157:H7 (ATCC43889) was purchased from ATCC (Manassas, MD). Biotin-anti-*E.*

78   *coli* antibodies was obtained from Meridian Life Science (Saco, ME) and dissolved in PBS

79   solution (pH=7.4). Bovine serum albumin (BSA), streptavidin (SA) and protein A were

80   purchased from Sangon Biotech (Shanghai, China). MacConkey agar, brain heart infusion (BHI)

81   culture medium were purchased from Becton, Dickinson and Company (Sparks, NV). PBS

82   solution containing 10 mM $K_3Fe(CN)_6$/$K_4Fe(CN)_6$ (Sangon Biotech., Shanghai, China) was used

83   for electrochemical measurements. Ultrapure water (18.2 MΩ cm) was obtained from a Millipore

84   Milli-Q purification system (Merck Millipore, MA).

85   The width of a finger and the gap between two fingers for SPIM (AIBIT Biotech Instrument,

86   China) are both 200 μm. One pair of gold electrodes and two welding plates were prepared on

87   ceramic base using screen-printed technology. Two electrodes were connected to the bonding

88   pad, respectively. The electrode contained multiple conducting ring with different diameter and

89   connected by conductive band. Fig S1 showed the details of the electrodes.

90   Electrochemical impedance spectroscopy (EIS) and cyclic voltammetry (CV) were

91   performed using ZAHNER electrochemical station (Kronach, Germany). Photosensitive resin

92   was purchased from DSM SOMOS Crop. (Somos imagine 8000, Elgin, IL). The devices with

93   different diameters (2r = 6, 7, 8 and 9 millimeter) were printed by a 3D printer (Liantai 450,

94   Shanghai, China) with 0.01 millimeter precision.

95   **2.2   Experimental methods**

96   2.2.1   Preparation of Bacterial Samples

97   *E. coli* O157:H7 was grown in BHI culture medium at 37 °C for 20 h to the stationary phase.

98   The stationary-phase cultures were diluted to 10^7–10^1 cfu·mL^{-1} in PBS (pH 7.4) and 100 μL of

99   the diluted solutions were transferred to MacConkey agar plates and incubated at 37 °C for 24 h

100   for enumeration of colonies. At the same time, the dilutions containing approximately 10^5

101   cfu·mL^{-1} of bacteria cells were prepared for evaluation of the proposed devices.

102   2.2.2   Dropping and immersing coatings

103   When the planar microelectrodes were incubated, the wide commonly used incubation

104   methods are dropping and immersing coatings for the incubation of planar microelectrodes.

105   Usually, the volume of dropping coatings is 10 to 50 μL, and the volume of immersing coating is

106   more than 1000 μL in order to cover the whole detection area. Generally, the droplet coverage

107   varies due to the discrepancy of the SPIMs surface. Figure 1 presents the droplets coverage of

108   electrode. The droplets coverage for the bare SPIM is significantly different, compared to that for

109   the modified SPIM (Fig S2).

110
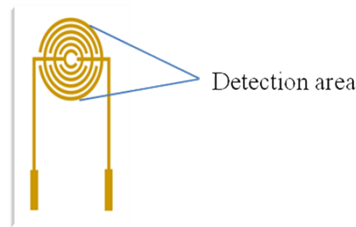
111   Figure 1. Detection area (Droplets area) of the electrode.

112   Furthermore, the droplets coverage may be changed during the modification process.

113   Several factors that might have caused this include surface tension, gravity, interface

114   hydrophobicity and the mobility of the molecules can be the reasons. In this experiment,

115   different treatment groups were set up as comparison. Treatment groups A and C were

116   immersing coating and treatment groups PBS and B were dropping coating, respectively. We

117   used 1500 µL PBS solution containing 50 µL protein A for coating (0.5 mg mL^{-1}) in treatment

118   group A, 50 µL protein A (0.5 mg mL^{-1}) in treatment group B, and 1500 µL protein A (0.5 mg

119   mL^{-1}) in treatment group C. The signal change was detected with EIS or CV techniques.

120   2.2.3   Nesting concept for incubation

121   In order to investigate the difference caused by the droplet coverage, we designed and

122   printed nest-like devices with different diameters. The devices (Figure 2) possess an equivalent

123   volume, but with different height and diameter (2r = 6, 7, 8 and 9 millimeter). The volume for

124   these nest-like devices was equivalent, which ensured the same concentration and quantity of

125   targets. The devices were incubated with BSA solution (2%, w/w) before use in order to avoid

126   the non-specific absorption. Two devices (2r = 6 and 9 millimeter) were selected to perform the

127   test to investigate the difference introduced by the multistep modification. The devices were used

128   to incubate SPIMs with SA solution (50 µL, 0.5 mg mL^{-1}) for 45 min and then biotin-antibody

129   was immobilized according to our previous research (Li et al., 2015a). After that, the bacteria

130   solution was added into the devices to incubate the SPIMs and the difference caused by multistep

131   modification was evaluated.
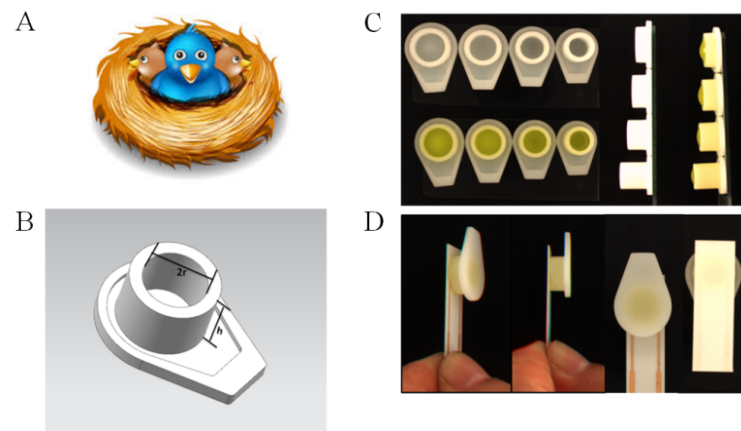
132

133   Figure 2. The 3D printed nest-like devices (B) with different height (h) and diameter (2r = 6, 7, 8 and 9 millimeter)
134   (C) and the photo of the incubation (D). The bird nest picture (A) was drew by Iconshock.

135   2.2.4   3D-printing ring devices

136   In the present research, both resin and glass were used to investigate the dispersity of the

137   target solution. A smart ring covered with silica gel was fabricated on the surface of the SPIM.

138   We used the nest-like devices with different diameters to cover the detection area and then use

139   silica gel to coat the devices. The caps were removed after the gel was completely dry, in order

140   to form a ring area. The ring can stay intact during the incubation and modification processes. In

141   order to prove that the rings are intact, solutions with different color were added into the devices

142   after each incubation and washing processes (Figure 3). The influence of NaOH solution was

143   also investigated for the cleaning process.
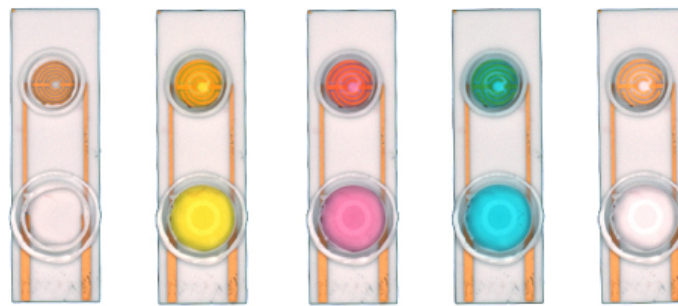
144

145   Figure 3. Silica gel ring on the surface of the SPIMs. Solution with different color were used to show the ring

146   concept(from left to right: no solution, solution with K^+, solution with Co^{3+}, solution with Cu^{2+}, ultrapure water).

147   On the basis of silica gel ring, we designed and printed ring devices with different diameters

148   (Figure 4). We selected two devices (2r = 6 and 9 millimeter) to investigate the performance. The

149   surface of these devices were also blocked with BSA solution to avoid non-specific absorption.

150   After that, these devices were fixed around of the detection area. The same amount of solution

151   was added into the devices to incubate SPIMs for 45 min. And then, the non-specific absorption

152   was washed with ultrapure water. The signal change was evaluated after the incubation.
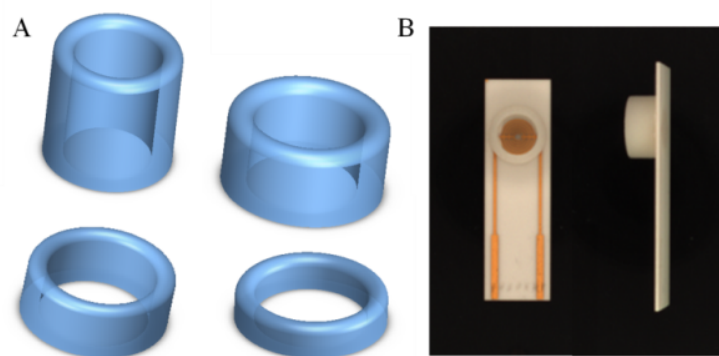
153

154   Figure 4. A) 3D printed ring devices with different diameters and B) SPIM with ring device to form a nest-like

155   device.

156   **2.3   Statistical Analysis**

157   Experiments were conducted in triplicates for each concentration level of protein A and

158   other materials. And bacteria cells were tested and the performance of the printed nest-like

159   devices with different diameters were collected. Statistical analysis were conducted using SPSS

160   17.0. The biosensor responses were considered to show significant difference when P-value was

161   less than 0.05 (95% confidence interval).

162   **3   Results and Discussion**

163   **3.1   Dropping and immersing coatings**

164   Four treatment groups were performed conducted and the application of PBS solution was

165   used as a control (Figure 5). Performances of treatment A and B were significantly different and

166   the signal change of treatment B was more obvious than that of treatment A. Treatment C

167   possessed more reactive molecules that can be captured on the surface of the devices in

168   comparison with treatment B. These results indicates that the signal changes are different

169   between immersing and dropping coatings. Since the two methods required different amount of

170   materials, it is not persuasive to conclude that the difference is caused by droplet coverage.

171
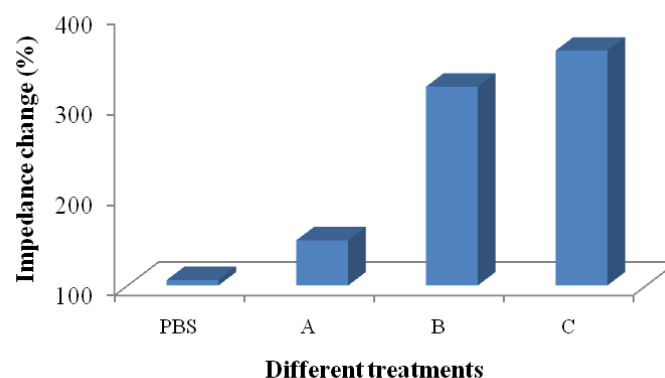
172   Figure 5. Immersing coating and dropping coating for the microelectrode modification. Treatment groups A and C
173   were immersing coating and treatment groups PBS and B were dropping coating. Treatment group A:1500 μL PBS

174 solution containing 50 µL of protein A (0.5 mg mL^{-1}); treatment group B:50 µL of protein A (0.5 mg mL^{-1});

175 treatment group C: 1500 µL of protein A (0.5 mg mL^{-1}).

3.2 Performance of nest-like devices

177 Considering the influence of the droplet coverage on the electrochemical response of SPIMs,

178 smarter design of devices is necessary. Nest-like devices with different diameters were used for

179 incubation (Figure 6). The results showed that there was significant difference between 9

180 millimeter and 6 millimeter devices ($p > 0.05$) and the difference were not significant for other

181 devices. According to the difference in the droplet coverage of these two devices, it can be

182 concluded that the signal response is influenced by droplet coverage.

183 In order to investigate the influence of the multistep modification, we selected 6 and 9

184 millimeters devices to perform the test for bacteria detection (Figure 7). Treatment group A was

185 prepared according to the signal change after SA modification. The results indicated that there

186 was significant difference between the devices ($p > 0.05$). Treatment group B (Figure 7) was

187 prepared according to the signal change of the bacteria incubation after the multistep

188 modification. The difference between the results collected from these two treatment groups did

189 not disappear. Due to the large dimension of the bacteria cells, not every site was occupied by

190 the bacteria cell. However, only effective absorption can introduce signal response. From the

191 results we concluded that the influence of droplets coverage was not disappeared by large

192 dimension of cells. Therefore, it is clear that the droplet coverage is an influencing factor for

193 electrochemical response.

194
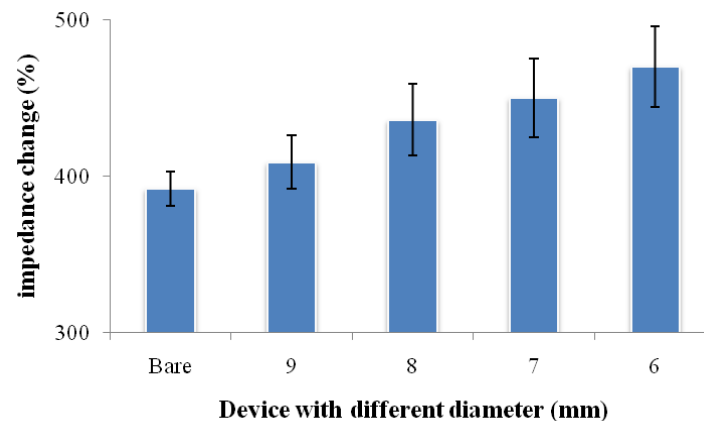
Figure 6. Signal change of the printed nest-like devices with different diameters for protein immobilization. Bare
was a SPIM without printed devices.

197
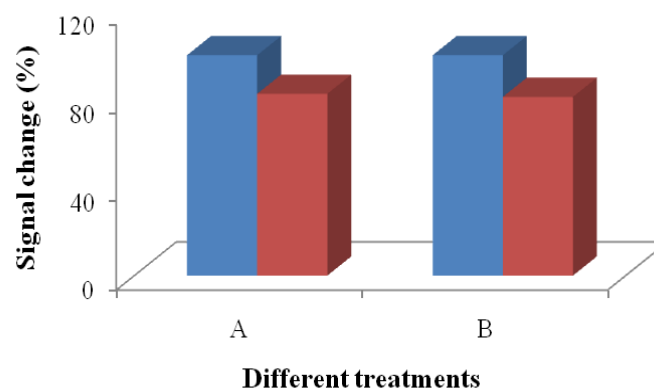
Figure 7. 3D printed nest-like devices (6 and 9 millimeters) for the test. Treatment group A was the performance
after SA modification. Treatment group B was the performance of the bacteria incubation, after the multi-step
modification.

3.3 Performance of silica gel ring

Resin and glass were used to investigate the dispersity of the target solution. The solution

coverage were different due to the different hydrophobicity of these two materials. However, the

surface constructed by these two materials was completely (or partly) damaged when washing

solution (NaOH, 1M) was used for SPIM regeneration. In order to deal with this situation, we

206   firstly designed a ring was prepared on the surface of SPIM using silica gel. The results indicated

207   that the signal was suppressed significantly compared to the treatment groups without the device,

208   considering that more molecules were immobilized effectively (Figure 8). Moreover, the

209   washing solution was available for this device without damage, indicating that the material and

210   device are both applicable.

211
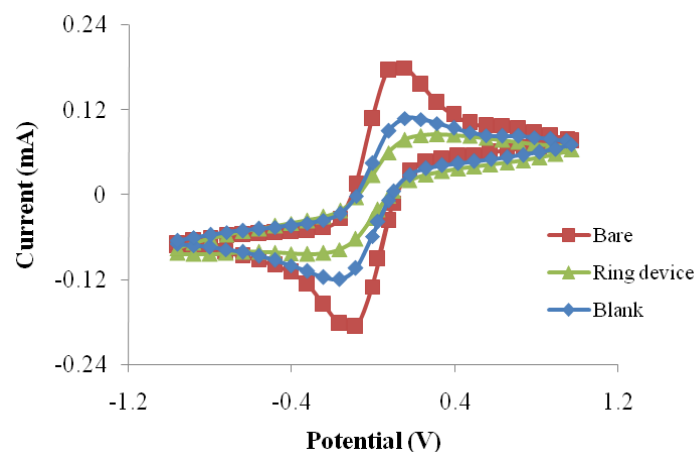
212   Figure 8. The CV performance of SPIMs with and without silica gel ring device.

213   **3.4   Performance of ring devices**

214   We designed and printed smart ring devices based on the concept of the silica gel ring. The

215   results in Figure 9 show that the immobilization of the protein gave rise to the EIS and CV signal

216   changes and the difference was significant between the two selected ring devices. The results

217   showed the decreases of peak currents of the electrochemical probe by 27% (9 mm) and 68% (6

218   mm), and the increases of impedance signal by 25% and 45%, respectively, indicating the

219   absorption was improved. Compared to the printed nest-like devices, less amount of materials is

220   required for ring devices. Moreover, it is useful to avoid the leakage of solution during the

221 process. It can reduce the evaporation as well, which is advantageous because avoid the irregular

222 signal change can be avoided. Moreover, the devices can be recycled to decrease the detection

223 cost because of no damage after an easy nondestructive cleaning process.
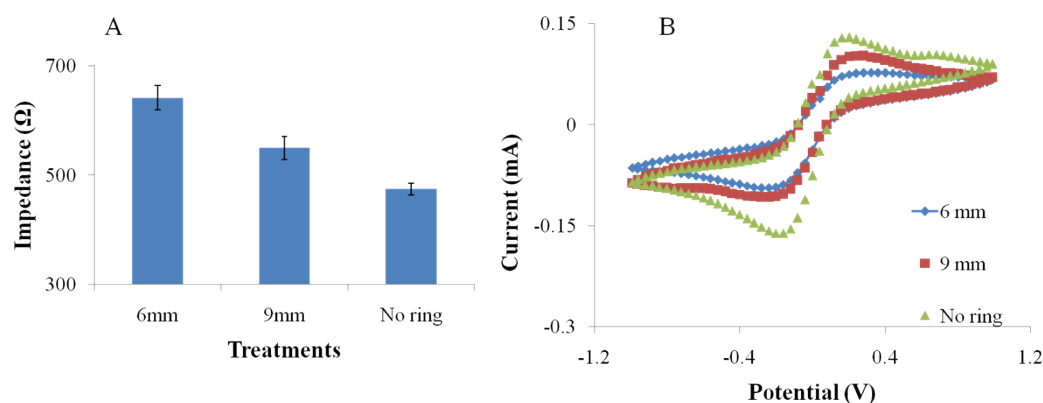
224

225 Figure 9. The EIS (A) and CV (B) performance of the SPIMs with and without 3D printed ring devices (6 and 9
226 millimeters).

227 **3.5   Base design using software**

228   Signal stability can be influenced by the droplet area. Different bases can be designed to

229 reduce the irregular signal. In this paper, we designed two bases using software (Figure 10) that

230 the droplets can be reserved within the scope of detection area. We used 3D printer to print the

231 base, verifying the application (Figure 11).
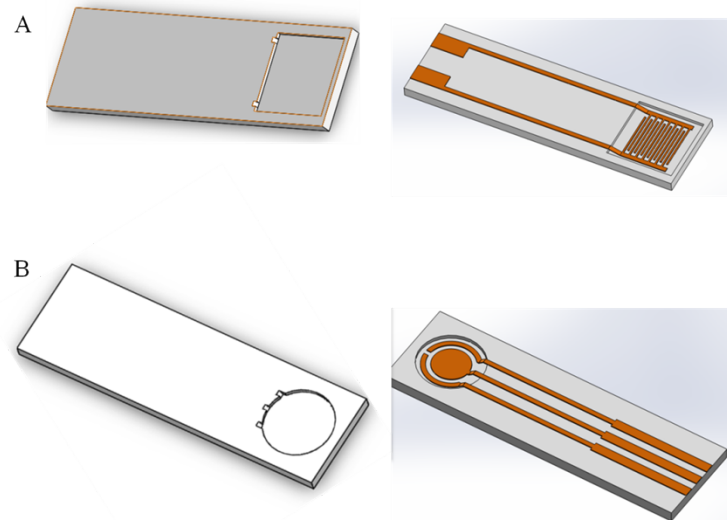
232

233 Figure 10. Two types of electrode bases designed by software. A) Interdigital microelectrode and B) Screen-
234 printed electrode.
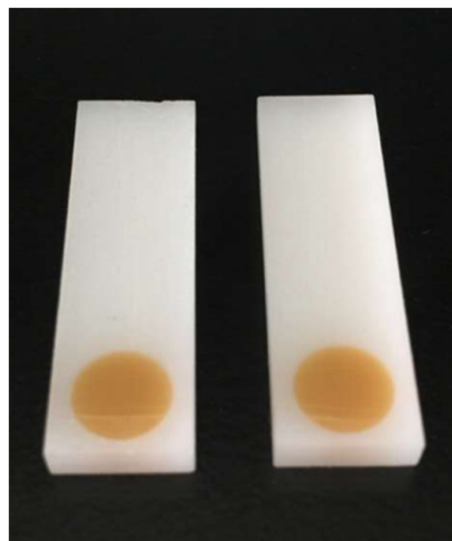
235
236   Figure 11. 3D printed base was used to verify the application.

237 **4   Conclusion**

238   In the present research, SPIMs was employed to evaluate the influence of droplets coverage

239 on the electrochemical response. 3D printing technology was used to print fabricate mini-small

240 smart devices with different diameters based on nesting concept. Nest-like devices with different

241 diameters (2r = 6, 7, 8, 9 millimeter) were designed and printed to construct achieve different

242 coverage to investigate the incubation performances and the results indicated that the influence

243 of coverage on electrochemical response was significant. Moreover, ring devices on the surface

244 of the SPIMs effectively improve the stability of the signal and also verify the such influence.

245 Detection cost can be greatly reduced by recycling of the printed devices. All the devices

246 improve the stability of the signal and eliminate the irregular signal change successfully. Our

247 proposed design and concept show great potential for application in the field of electrodes

248 fabrication and stable electrochemical biosensors construction.

249 **Acknowledgments**

250 The authors thank Biosensing & Biomodeling Lab at Zhejiang University for their support of the

251 electrodes and electrochemical station. We gratefully acknowledge Muyang Lin and Xi Yu

252 (College of Chemistry, National University of Singapore) for their help.

253 **References**

254 Bernalte, E.; Sánchez, C.M.; Gil, E.P. 2011. Determination of mercury in ambient water samples by anodic
255 stripping voltammetry on screen-printed gold electrodes. *Anal. Chim. Acta*, 689(1), 60-64.
256 Brett, C.M.A.; Thiemann, C. 2002. Conducting polymers from aminobenzoic acids and
257 aminobenzenesulphonic acids: Influence of ph on electrochemical behaviour. *J. Electroanal. Chem.*, 538–539,
258 215-222.
259 Ch, S.; Jenke, M.; Hoffmann, P.; Brugger, J. 2006. Interdigitated 50 nm ti electrode arrays fabricated using xef
260 2 enhanced focused ion beam etching. *Nanotechnology*, 17(11), 2722.
261 Costa, R.; Pereira, C.M.; Silva, A.F. 2015. Charge storage on ionic liquid electric double layer: The role of the
262 electrode material. *Electrochim. Acta*, 167, 421-428.
263 Gerard, M.; Chaubey, A.; Malhotra, B.D. 2002. Application of conducting polymers to biosensors. *Biosens.*
264 *Bioelectron.*, 17(5), 345-359.
265 Gryczan, P.; Kisiel, A.; Michalska, A.; Maksymiuk, K. 2015. Electrochemical properties of polypyrrole doped
266 by alternating polymer micelles. *Electroanalysis*, 27(3), 752-759.
267 Huang, X.; O'Mahony, A.M.; Compton, R.G. 2009. Microelectrode arrays for electrochemistry: Approaches to
268 fabrication. *Small*, 5(7), 776-788.
269 Huey, E.; Krishnan, S.; Arya, S.K.; Dey, A.; Bhansali, S. 2012. Optimized growth and integration of silica
270 nanowires into interdigitated microelectrode structures for biosensing. *Sensors and Actuators B: Chemical*,

271 175, 29-33.

272 Hunt, H.K.; Armani, A.M. 2010. Label-free biological and chemical sensors. *Nanoscale*, 2(9), 1544-1559.

273 Kostecki, R.; Song, X.Y.; Kinoshita, K. 2000. Influence of geometry on the electrochemical response of
274 carbon interdigitated microelectrodes. *J. Electrochem. Soc.*, 147(5), 1878-1881.

275 Lepinay, S.; Staff, A.; Ianoul, A.; Albert, J. 2014. Improved detection limits of protein optical fiber biosensors
276 coated with gold nanoparticles. *Biosens. Bioelectron.*, 52, 337-344.

277 Li, Z.; Fu, Y.; Fang, W.; Li, Y. 2015a. Electrochemical impedance immunosensor based on self-assembled
278 monolayers for rapid detection of escherichia coli o157:H7 with signal amplification using lectin. *Sensors*
279 *(Basel)*, 15(8), 19212-19224.

280 Li, Z.; Yu, Y.; Li, Z.; Wu, T. 2015b. A review of biosensing techniques for detection of trace carcinogen
281 contamination in food products. *Anal. Bioanal. Chem.*, 407(10), 2711-2726.

282 Liu, J.; Wagan, S.; Dávila Morris, M.; Taylor, J.; White, R.J. 2014. Achieving reproducible performance of
283 electrochemical, folding aptamer-based sensors on microelectrodes: Challenges and prospects. *Anal. Chem.*,
284 86(22), 11417-11424.

285 Olaru, A.; Bala, C.; Jaffrezic-Renault, N.; Aboul-Enein, H.Y. 2014. Surface plasmon resonance (spr)
286 biosensors in pharmaceutical analysis. *Crit. Rev. Anal. Chem.*, 45(2), 97-105.

287 Park, S.; Beskok, A. 2008. Alternating current electrokinetic motion of colloidal particles on interdigitated
288 microelectrodes. *Anal. Chem.*, 80(8), 2832-2841.

289 Santoro, C.; Guilizzoni, M.; Correa Baena, J.P.; Pasaogullari, U.; Casalegno, A.; Li, B.; Babanova, S.;
290 Artyushkova, K.; Atanassov, P. 2014. The effects of carbon electrode surface properties on bacteria attachment
291 and start up time of microbial fuel cells. *Carbon*, 67, 128-139.

292 Sun, J.; Zhou, W.; Huang, D.; Fuh, J.H.; Hong, G. 2015. An overview of 3d printing technologies for food
293 fabrication. *Food Bioprocess Technol*, 8(8), 1605-1615.

294 Taleat, Z.; Khoshroo, A.; Mazloum-Ardakani, M. 2014. Screen-printed electrodes for biosensing: A review
295 (2008–2013). *Microchim. Acta*, 181(9-10), 865-891.

296 Thévenot, D.R.; Toth, K.; Durst, R.A.; Wilson, G.S. 2001. Electrochemical biosensors: Recommended
297 definitions and classification1. *Biosens. Bioelectron.*, 16(1–2), 121-131.

298 Ueno, K.; Hayashida, M.; Ye, J.-Y.; Misawa, H. 2005. Fabrication and electrochemical characterization of
299 interdigitated nanoelectrode arrays. *Electrochem. Commun.*, 7(2), 161-165.

300 Valentini, F.; Ciambella, E.; Conte, V.; Sabatini, L.; Ditaranto, N.; Cataldo, F.; Palleschi, G.; Bonchio, M.;
301 Giacalone, F.; Syrgiannis, Z.; Prato, M. 2014. Highly selective detection of epinephrine at oxidized single-wall
302 carbon nanohorns modified screen printed electrodes (spes). *Biosens. Bioelectron.*, 59, 94-98.

303 Van Dorst, B.; Mehta, J.; Bekaert, K.; Rouah-Martin, E.; De Coen, W.; Dubruel, P.; Blust, R.; Robbens, J.
304 2010. Recent advances in recognition elements of food and environmental biosensors: A review. *Biosens.*
305 *Bioelectron.*, 26(4), 1178-1194.

306 Vilé, G.; Albani, D.; Nachtegaal, M.; Chen, Z.; Dontsova, D.; Antonietti, M.; López, N.; Pérez‐Ramírez, J.
307 2015. A stable single‐site palladium catalyst for hydrogenations. *Angewandte Chemie International Edition*,
308 54(38), 11265-11269.

309 Wang, Y.; Ye, Z.; Ying, Y. 2012. New trends in impedimetric biosensors for the detection of foodborne
310 pathogenic bacteria. *Sensors*, 12(3), 3449.

311 Wei, X.; Li, D.; Jiang, W.; Gu, Z.; Wang, X.; Zhang, Z.; Sun, Z. 2015. 3d printable graphene composite.

312 *Scientific Reports*, 5, 11181.

313 Xing, J.; Zheng, M.; Duan, X. 2015. Two-photon polymerization microfabrication of hydrogels: An advanced

314 3d printing technology for tissue engineering and drug delivery. *Chem. Soc. Rev.*, 44(15), 5031-5039.

315 Xu, J.; Bao, N.; Xia, X.; Peng, Y.; Chen, H. 2004. Electrochemical detection method for nonelectroactive and

316 electroactive analytes in microchip electrophoresis. *Anal. Chem.*, 76(23), 6902-6907.

317 Zhu, J.; Zhou, Y.; Gao, C. 1998. Influence of surfactants on electrochemical behavior of zinc electrodes in

318 alkaline solution. *J. Power Sources*, 72(2), 231-235.

319